Molecular Crystals and Liquid Crystals
Publication details, including instructions for authors and subscription information:
http://www.tandfonline.com/loi/gmcl16

# Dielectric Behaviour and Molecular Motion in Low-Temperature Phase of t-Nitrobutane (TBN)

P. Freundlich [a] & L. Sobczyk [a]
[a] Institute of Chemistry University of Wroclaw, Wroclaw, 50-383, Poland.
Version of record first published: 20 Apr 2011.

To cite this article: P. Freundlich & L. Sobczyk (1981): Dielectric Behaviour and Molecular Motion in Low-Temperature Phase of t-Nitrobutane (TBN), Molecular Crystals and Liquid Crystals, 65:3-4, 197-214

To link to this article: http://dx.doi.org/10.1080/00268948108082134

*Mol. Cryst. Liq. Cryst.*, 1981, Vol. 65, pp. 197–214
0026-8941/81/6504-0197$06.50/0

Printed in the U.S.A.



# Dielectric Behaviour and Molecular Motion in Low-Temperature Phase of t-Nitrobutane (TBN)

P. FREUNDLICH and L. SOBCZYK
*Institute of Chemistry, University of Wrocław, 50–383 Wrocław, Poland.*

(*Received April 18, 1980*)

Low-temperature phase transition at 215 K in *t*-nitrobutane is accompanied by considerable jump of electric permittivity. Measurements of $\varepsilon^*(T)$ in microwave region and calculated correlation functions, by using additionally data on $\alpha(\omega)$ in far infra-red, allow to conclude that the permittivity jump is due to the change of the potential energy shape for librations perpendicular to the polar axis of molecules. It has been shown that dielectric losses can be ascribed to the low-frequency wing of the absorption band which during phase transition is shifted towards higher frequencies.

## INTRODUCTION

The compounds of the general formula $(CH_3)_3CX$ where X = Cl, Br, $NO_2$, CN exhibit two phase transitions below the melting point which are related to retardation of rotational motions. In spite of structural similarities and considerable analogies in phase transitions, particularly with respect to changes in molal heat capacities, each of the 4 compounds mentioned above exhibits specific properties which are demonstrated in a peculiar way in its dielectric properties (cf. Table I). Nitro-*t*-butane is distinguished by the fact that apart from a large decreasing of $\varepsilon'$ in the phase I-phase II transition resulting from the freezing of free rotation, it exhibits a second decreasing of $\varepsilon'$ in the II-III transition whose nature has not been fully understood. A similar decreasing of $\varepsilon'$ is found for cyanobutane but in the I-II transition; this compound loses its freedom of rotation during freezing which is most probably related to the highest asymmetry of its molecules.

In our previous report[16] we have suggested that the low-temperature phase transition is related to the stepwise change of librational motions of the dipoles, describing phase II as a "librational" one. On the other hand,

TABLE I

Properties and phase transitions of $(CH_3)_3CX$ compounds

| | | X = Cl | Br | $NO_2$ | CN |
|---|---|---|---|---|---|
| Dipole moment in gas phase × $10^{30}$ cm | | 7.12[2] | 7.36[2] | 12.35[3] | 13.15[4] |
| asymmetry parameter[a] | | 1.00 | 1.09 | 1.07 | 1.18 |
| | Freezing temperature, K | 248.4[5,6] | 256.2[2] | 299.2[7] | 292.1[8] |
| | Crystallographic system | fcc[9] | fcc[10] | ortho-rhombic[5] | tetragonal[11] |
| | Packing factor | 0.59 | 0.60 | 0.59 | 0.58 |
| Phase I | $\Delta S$ at transition to phase II, J/mol·K | 25.83[13] | 4.61[5] | 17.92[7] | 7.79[8] |
| | Dielectric increment, $\Delta S$, at the transition to phase II | 12.8[13,14] | 1.7[15] | 24.2[16] | 0.45[17] |
| | Transition temperature (I–II), K | 219.4[5,6] | 231.5[5] | 260.1[7] | 232.7[8] |
| | Crystallographic system | tetragonal[9] | ortho-rhombic[2] | triclinic[7] | ? |
| | Packing factor | 0.63 | 0.62 | 0.61 | ? |
| Phase II | $\Delta S$ at the transition to phase III J/mol · K | 10.17[13] | 27.2[5] | 19.64[7] | 1.09[8] |
| | Dielectric increment, $\Delta\varepsilon$, at the transition to phase III | 0.15[5] | 8.8[15] | 0.8[16] | 0.0[17] |
| | Transition temperature (II–III), K | 183.1[5,6] | 208.7[5] | 215.3[7] | 213.0[8] |
| Phase III | Crystallographic system | ortho-rhombic[2] | ortho-rhombic[2] | triclinic[7] | ? |
| | Packing factor | 0.68 | 0.68 | ? | ? |

[a] Acc. to Smyth.[1]
[b] Acc. to Kitaigorodsky.[12]

QNS studies[11] have shown that during the low-temperature transition uniaxial rotations become frozen along the polar axes of molecules. However, such freezing could not affect permittivity. It is not unlikely that in this transition both uniaxial rotation is retarded and the shape of the librational motion potential varies. For better understanding of low-temperature phase transitions in $(CH_3)_3CX$ compounds we have decided to carry out dielectric studies over a broad frequency range, to compare them with absorption measurements in the far infra-red which is most probably related to libration vibrations and to obtain a consistent pattern of dielectric response, from static polarization through the micro-wave region up to the far infra-red frequencies.

## EXPERIMENTAL

Specific properties of TBN as a typical plastic crystal, i.e. a low heat of evaporation and sublimation at the high vapour pressure and relatively high changes in density during solidification result in the formation of a characteristic "vapour snakes."[18] Macroscopic heterogeneity of the sample renders it difficult to achieve reproducible results of electric measurements.

In order to obtain accurate results of $\varepsilon^*$ measurements it was necessary to apply such a technique and such equipment to carry out measurements on possibly small samples of strictly determined dimensions to reduce down to a minimum improper packing of the sample.

### a Static measurements 500 kHz

Measurements were carried out by the heterodyne-beat method in a thermostat-controlled two-electrode coaxial capacitor designed so that to prevent any variation in active capacitance during solidification. It may be filled with a small quantity of substance (about 3 cc) in spite of its relatively high active capacitance $C_0$ (about 16 pF). A precise Sullivan 70100 air capacitor of a linear characteristic in the 300 pF range and $2 \cdot 10^{-2}$ pF accuracy of reading or a General Radio capacitor with the 1050 pF range (deviation from linearity below 0.1 pF) and 0.1 pF accuracy of reading were used as standard capacitors. The former capacitor was used to determine the thermal dependence of capacitance for an empty and standard-filled capacitor.

The maximum measuring error[19] depends, on accuracy of reading of the standard capacitor and ranges from $\pm 0.04$ for $\varepsilon_0 = 3$ to $\pm 0.4$ for $\varepsilon_0 = 30$ for a capacitor with the 1050 pF range. A temperature-control system maintained the temperature in the 180–450 K interval accurate to

$\pm 0.05$ K which enabled us to determine the freezing point of TBN with an accuracy of 0.1 K (stepwise increase in permittivity).

It appeared important to form the sample in phase I, free from bubbles and cavities. Reproducibility of capacitance measurements for a capacitor filled with solid TBN was taken as a correctness measure of this process.

The sample was repeatedly cooled down to about 250 K (below the rotational transition) and then was heated up very slowly (1–2 K per hour) to about 290 K with $\varepsilon_0(T)$ measurements performed during all this period. Reproducible values of permittivities, independently of the direction of temperature changes, are also the highest obtainable $\varepsilon_0$ values which is evidence of the maximum sample packing.

### b Microwave measurements at 1.984 GHz

Measurements at this frequency were carried out in the coaxial line by the so-called lumped capacitance method described in detail by Kołodziej *et al.*[20] The sample is formed in a transparent ring stuck to the top part of the inner conductor (Figure 1). Ring (3) made of Pyrex glass, wall thickness below 0.25 mm and specially polished (dimensional tolerances below 5 $\mu$m) was closed from the top by means of a metal cap (1) provided with a hole to remove bubbles during the filling of the ring with standard liquid for the calibration process. The cap adhered to membrane (2) of copper or aluminium foil. Proper contact was ensured by constant pressure of spring (10) against the membrane through piston (11).

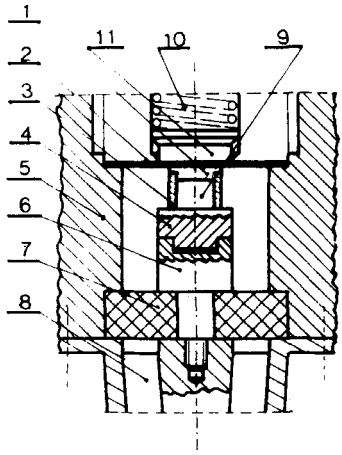


FIGURE 1 Termination of a coaxial wave-guide in the capacitance method, 1–closing diaphragm, 2–membrane, 3–glass ring, 4–plug terminal, 5–outer conductor, 6–socket terminal, 7–dielectric bracket (teflon), 8–conic passage, 9–sample, 10–spring, 11–piston.

Calibration of the system was performed at 298 K by means of two standards, a lossless one (air) and dichloroethylene.

Repeatability of measurements was ensured by observing the optimum cooling rate found to be 10 K/hour.

The sample was formed by means of a special mould to prevent any damage to the ring. The base (item 4 in Figure 1) with a ring stuck to it was placed on the cooling plate. A few drops of the substance was introduced from a pipette and by pressing the teflon piston the ring was filled gradually. Excess substance was removed through a cap hole (item 1) by heating it up slightly.

Optical transparency of the ring permits to check if the sample is properly formed. The sample formed in this way, in most cases a transparent one, was placed in a sample holder cooled down below the freezing point of the sample. Measurements of the standing wave minimum ($l_{min}$) and double minimum widths $\Delta x$ for each temperature were repeated several times (for low-loss samples, e.g. in phase II, about ten times). The values of total errors estimated by means of computer analysis for a single measurement in this method are summarized in Table II.

TABLE II

Maximum error of single measurement in the capacitance method

| | Measured values | Maximum error (absolute) |
|---|---|---|
| $\varepsilon'$ | 26.71 | $\pm 0.56$ |
| | 19.71[a] | $\pm 0.41$ |
| | 3.32 | $\pm 0.12$ |
| $\varepsilon''$ | 3.55 | $\pm 0.22$ |
| | 1.90[a] | $\pm 0.13$ |
| | 0.07 | $\pm 0.05$ |

[a] Results obtained for cyano-*t*-butane in liquid phase.

The systematic error of $\varepsilon'$ and $\varepsilon''$ measurements was estimated in the lumped capacitance method by means of known complex permittivity standards. For 1,2-dichloroethylene the values of $\varepsilon'$ and $\varepsilon''$ measured at 1.984 GHz were 9.86 and 0.745, respectively. The corresponding reference values[21] are 10.04 and 0.729, i.e. the systematic error does not exceed 1.5%.

### c Microwave measurements at 38.09 GHz

These measurements were performed by the reflection method for a short-circuit rectangular wave-guide.[22]

The main source of the impedance discontinuities in the wave-guide line are a large number of connections, which lead to the field distribution near the standing wave minimum. For this reason SWR was measured by means of two connected in series 0–30 dB variable precision attenuators. Additionally the effect of the detection diode characteristic was eliminated also.

A large number of connections and considerable distances between the sample and probe required an allowance to be made for the losses of the line itself as well as for additional reflections resulting from impedance discontinuities. The dependence of losses on the probe position was determined by the movable short-circuit method whereas the position of the reference plane related to reflections from the connectors and particularly from the terephthalate-foil window was determined by calibration by means of lossless standards (polystyrene, teflon and TBN in the phase frozen at 140 K).

During preliminary measurements the conditions of stabilization of thermal equilibrium were fixed (by measuring the reference plane position, for a plate-short wave-guide, depending on temperature).

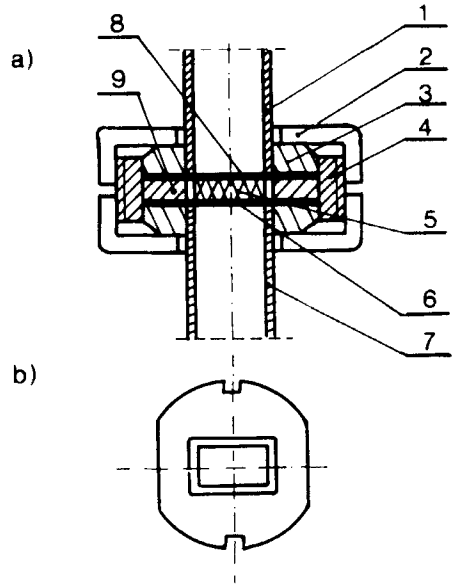


FIGURE 2 Sample mounting in the wave-guide. (a) Mutual positions of particular components: 1–top wave-guide section, 2–top nut, 3–wave-guide joint, 4–tapped centring sleeve, 5–sample, 6–foil window, 7–inner wave-guide, 8–short-circuit plate, 9–sample holder; (b) Top view of the sample holder (9).

The sample was moulded in a similar manner to that described earlier, in a specially cut wave-guide section, 2.00 ± 0.005 mm or 0.75 ± 0.005 mm thick, terminated from one end with a thin metallic plate, and on the other end, on connecting to the slotted line, with a terephthalate-foil window 50 ± 1 $\mu$m thick (Figure 2).

The moulding process performed outside the measuring head facilitated a control of the wave-guide filling degree and surface quality of the sample.

The moulded sample was put into the cell cooled down to about 285 K and the temperature was reduced keeping the condition settled previously (cooling rate was about 10 K/hour).

With a properly moulded sample and well pressed down foil window, the sample removed after the full measuring cycle is completed (25–36 hours) was still fully transparent and showed no losses of mass. Measuring accuracy of permittivity and dielectric losses in the reflection method depends on measuring errors of the sample thickness, standing wave ratio SWR of the line with sample, SWR of the empty line, wavelength inside the wave-guide and the shift of minimum, Δ.

TABLE III

Maximum error of a single measurement in the reflection method

| | Measured magnitudes (approximate values) | Maximum error (absolute) |
|---|---|---|
| $\varepsilon'$ | 6.5 | ±1.0 |
| | 3.1 | ±0.14 |
| | 2.5 | ±0.14 |
| $\varepsilon''$ | 7.5 | ±0.50 |
| | 0.15 | ±0.02 |
| | 0.01 | ±0.01 |

The most important source of measuring errors is misfit of the sample thickness, $d$, to the wavelength in the sample, $\lambda_2$. If the $d/\lambda_2$ ratio is close to 0.25, the lowest errors are observed for $\varepsilon''$ whereas the lowest errors for $\varepsilon'$ occur at $d/\lambda_2$ close to 0.5. Measuring errors summarized in Table III, determined as previously by means of computer analysis, apply to the most unfavourable case.

On measuring $\varepsilon'$ the accuracy is critically affected by measurements of the thickness and Δ. On measuring $\varepsilon''$ particularly for low losses, the errors made on determining SWR of both the empty line and that filled with the sample are predominant.

## RESULTS AND DISCUSSION

The results of measurements in the form of plots of static permittivity $\varepsilon_0$ versus temperature and both complex permittivity components of TBN (at 2 and 38 GHz) are summarized in Figures 3 and 4. Full lines in the figures are drawn through the points corresponding to the arithmetic means of measurements at a given temperature for all measuring series, one series containing the results of measurements obtained on one sample, i.e. on one filled ring or one condenser filling. Measurements were performed (except for static permittivity) only during the cooling down process. The continuous static permittivity curve was drawn only for the points measured on decreasing the temperature.

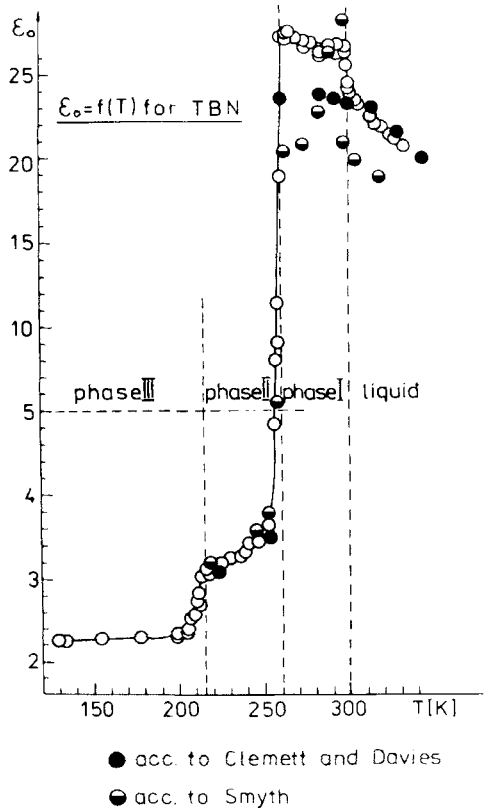


FIGURE 3 Static permittivity of TBN (500 kHz). ●–Clemett and Davies,[23] ◒–Crowe and Smyth[24].

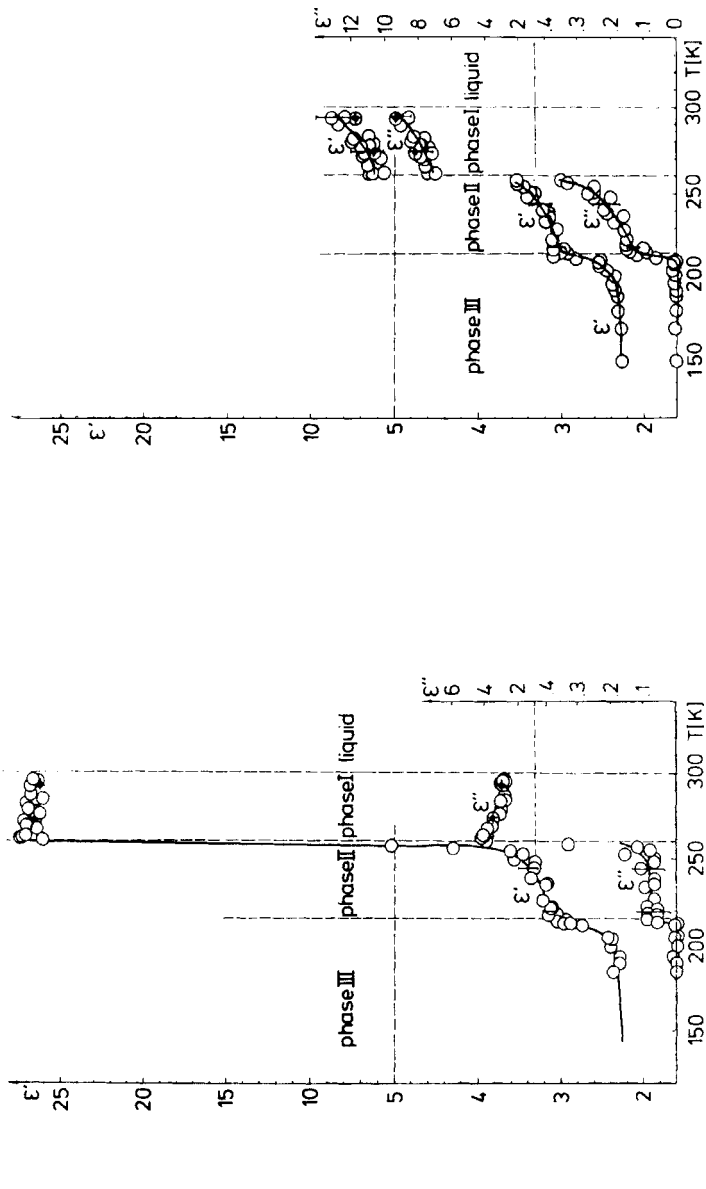


FIGURE 4 Complex permittivity $\varepsilon^*$ of solid TBN (a) at 2 GHz, (b) at 38 GHz. Vertical dashes denote error intervals; ◆ Urban's results.

### a Static permittivity measurements

The three phase transitions shown in Figure 3—solidification at 299 K, rotational transition at 260 K and transition at 215 K separate, in turn, the liquid, rotational (I), librational (II) and frozen (III) phases in the dielectric sense.[16]

The value of $\varepsilon_0$ found for phase III is close to $n_D^2$ and using it as $\varepsilon_\infty$ leads to a very high contribution (as compared with the molar refraction $R_D$ = 26.2 cm$^3$) of molecular atomic polarizability $P_A = 5.7 - 6.5$ cm$^3$ which is in very good agreement with $P_A = 6.1$ cm$^3$, quoted by Wiswall and Smyth.[3]

The permittivity in phase I differs from that measured by Clemett and Davies[23] and Smyth.[24] Presumably it is connected with the kind of treatment of the sample.

Then as additional factor may be the presence of impurities which results in the freezing point depression of TBN by about 2.5 K.[24] It appeared during preliminary measurements that the method of sample moulding and the presence of impurities have no significant influence on the temperature of rotational phase transition and permittivity in the lower temperature phases; hence, the results of this paper are in full agreement with Smyth and Clemett's measurements in phase II (Figure 3).

A low increase of the dipole correlation factor $g$ during solidification as mentioned in Ref. 16 ($g = \mu_{\text{off}}^2/\mu_{\text{gas}}^2$) may result from the existence of small and short-living domains "microstructures" near the freezing point which are the source of an additional dipole moment. A decrease in the correlation factor in phase I may result from the potential distribution for rotation existing in this phase around the axis perpendicular to the dipole moment direction which may be approximated by the two-well model. This was suggested by Urban[2,25] who analyzed the shapes of molecules and measured dielectric relaxation in the liquid and plastic phases. The difference in depths of both wells determined by him from the Meakins relation[26]

$$\varepsilon_0 - \varepsilon_\infty = \frac{C}{T}\left(1 + \cos \mathrm{h}\,\frac{Q}{RT}\right)^{-1}$$

(where $C$ is constant) is 2.1 $\pm$ 0.4 kJ/mole and, being comparable with the value of $RT$ in this temperature range (2.2–2.5 kJ/mole), does not affect significantly the freedom of reorientation in this phase, particularly near the freezing point.

A change in the crystallographic system during the phase transition at 260 K from the orthorhombic system of lattice parameters similar to those of the cubic system into the triclinic system whose parameters differ only slightly from those of the tetragonal system[2,7] should be accompanied by a change in the shape of the potential energy curve during rotation.[27] One

of its effects is a shift of the absorption band maximum $\alpha$ found in the far infra-red[28] from 33 $cm^{-1}$ in the plastic phase to 65 $cm^{-1}$ in phase II.

A plot of static permittivity versus temperature for TBN in phase II near 260 K is fairly well consistent with the Fröhlich model for an ordered crystal. The initial considerable decrease in permittivity results from some molecules being "frozen" at lower energy equilibrium positions which involves an increase in the difference in depths of both wells.

Assuming that in phase II the activation barrier $\Delta H$ for isotropic reorientation was raised considerably (as compared to about 4.4 kJ/mole in the plastic phase,[25] any further course of variations in $\varepsilon_0(T)$ may be explained as due to librations performed by the molecules inside the potential well around the axis perpendicular to the dipole moment sense.[29,30]

In this phase, as shown by QNS measurements,[11] the TBN molecules are simultaneously liable to rotate uniaxially around the C–N bond. Overlapping of both types of motion causes that under the influence of the electric field applied the mean value of the $\Theta$ angle[16] differs from zero.

On this assumption one can formulate[16,30] an expression relating the libration frequency $\omega$ to the magnitude of molar polarizability according to equation[16]

$$P_{\text{libr}} = \frac{2}{9} \frac{N_A \mu_v^2}{I \omega_0^2 \varepsilon^0}$$

where $I$ is the moment of inertia and $\mu_v$ is the dipole moment of a free molecule.

Molar polarizability of TBN determined from dielectric measurements (using Onsager relation) in phase II is 13.2 $cm^3$ at 219 K and 16.4 $cm^3$ at 244 K. Taking into calculations $\mu_v = 12.37 \cdot 10^{-30}$cm and $I = 372 \cdot 10^{-47}$ $kgm^2$, the estimated libration frequency is 36 and 33 $cm^{-1}$, respectively, and is almost half as low as that determined from the maximum position of absorption coefficient $\alpha$ at these temperatures.[28] Because of the simplicity of the above model and assumptions taken (polycrystalline sample, harmonic potential) this agreement should be considered satisfactory.

During transition at 215 K to phase III, the uniaxial rotation rate decrease rapidly (below detectability of the QNS method.)[11] The absence of rotation and libration overlapping might suggest that $\langle\Theta\rangle = 0$ and thus the contribution to libration polarizability disappears.

A stepwise change in the $\varepsilon_0(T)$ function found in this phase transition may also be explained by assuming that the dielectric increment in phase II $(\varepsilon_0 - n_D^2)$ is related to relaxation of some molecules exhibiting freedom of reorientation owing to the existence of various types of defects in the TBN crystal. A considerable depth of the well and absence of any visible dependence of the permittivity value in phase II and III on the freezing method indicate

that such an explanation of the $\varepsilon_0(T)$ plot seems to be very unlikely. One could have expected that more detailed information on this problem will be supplied by studies of $\varepsilon^*$ at high field frequencies.

### b Results of measurements in the microwave range

The plots of complex permittivity versus temperature for the 1.984 and 38.09 GHz frequencies rule out the existence of any maximum for the reorientation processes of the TBN molecules at frequencies below 38 GHz. On the contrary, low losses $\varepsilon'' = 0.13$ at 219 K and 0.22 at 244 K at 38 GHz (as compared with the magnitude of dielectric increment—0.92 and 1.14, respectively) suggest the existence of a maximum at much higher frequencies. In the plastic phase the maximum absorption related to reorientation of the entire molecule occurs in the 10–22 GHz region so one can hardly expect that this process would take place at a much higher frequencies in the lower temperature phase. This indicates that absorption related to the dielectric increment of TBN in phase II has a resonance nature and may be assigned to the librational motion of the molecule in combination with simultaneous rapid uniaxial rotation.

Thus, dielectric manifestations in the microwave region in such a formulation should be consistent with the absorption spectrum in the far infra-red. In the far infra-red range a broad absorption band is found which is assigned to the librational motion. Taking the results of measurements in the microwave region ($<2$ cm$^{-1}$) and absorption curve in the far infra-red[28] as a starting point, the dependence of $\varepsilon'$ and $\varepsilon''$ *versus* frequency was estimated in the 0.001–160 cm$^{-1}$ range by means of a scheme based upon the Kramers–Kronig relation. For calculation of the main integral value the method of parabolae suggested by Hawranek[31] was applied. During each run the values of dispersion $\varepsilon_0 - \varepsilon_\infty$ were compared. Computations were interrupted when the differences between successive values did not exceed the preset value (0.02). As a selection criterion of $\alpha(\tilde{\nu})$ in the intermediate range (40 GHz–20 cm$^{-1}$) between the results of microwave measurements and in the far infra-red (Figure 5) the condition of monotonic plot $\varepsilon'(\tilde{\nu})$ in this range was assumed. The value of $\varepsilon_\infty$ determined in this manner (knowing $\varepsilon_0$[16] from the static measurements) is similar to the magnitude obtained from the measurements of temperature dependence. Error of estimate for $\alpha(\tilde{\nu})$ in the range of interpolation does not exceed 5%. Scheme of calculations is presented in Figure 6.

The plots of $\varepsilon'$ and $\varepsilon''$ against frequency for particular phases are presented in Figures 7 and 8. These results seem to indicate that in fact, the high-frequency ranges of the absorption bands and the resulting dispersion curves and dielectric data are in full agreement.

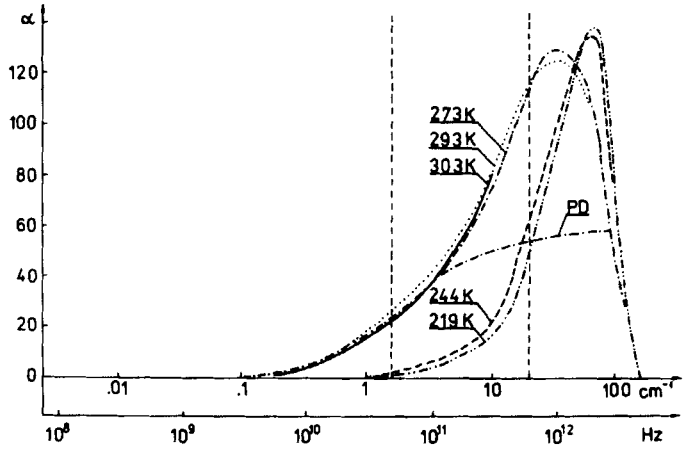


FIGURE 5 Absorption coefficient α versus frequency for TBN in liquid phase (303 K), in phase I (273 and 293 K) and in phase II (219 and 244 K); PD-Debye plateau (273 K).

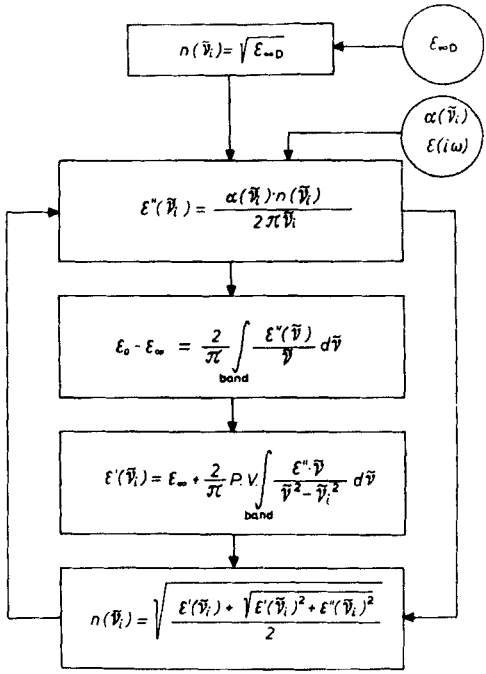


FIGURE 6 Calculation diagram of $\varepsilon'$ and $\varepsilon''$ versus frequency over the whole absorption region (microwave range and far infra-red) P.V.—principal value of the integral.

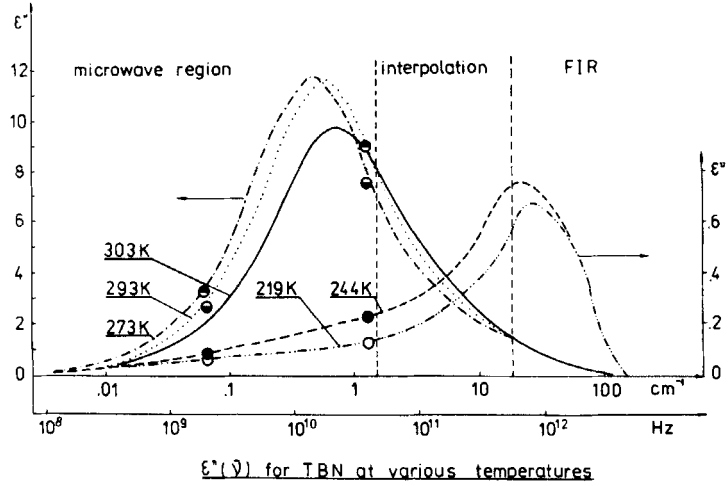


FIGURE 7 Dielectric losses $\varepsilon''$ versus frequency for TBN. Denotations as in Figure 5. In the microwave region the curves for liquid phase and phase I were determined by means of Debye distribution parameters;[25] O–experimental points.

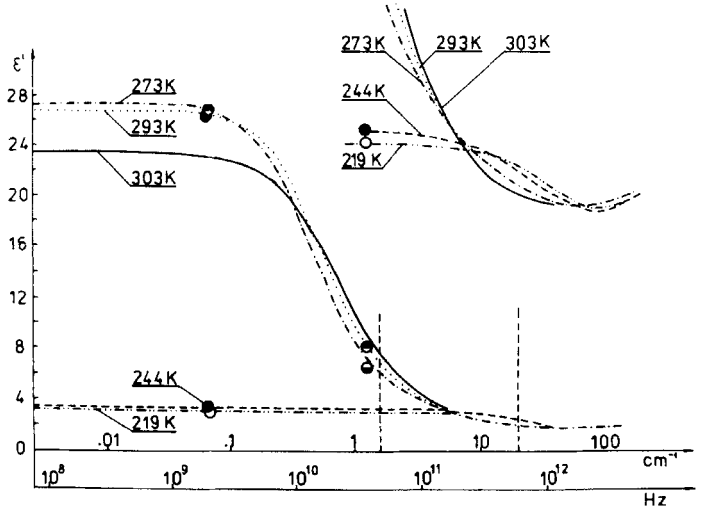


FIGURE 8 Dielectric permittivity $\varepsilon'$ of TBN determined by means of Kramers–Kronig relation. Denotations as in Figure 5. O–experimental points.

### c Correlation functions

Utilization of the correlation function formalism creates an additional possibility for distinction between the activation and libration absorption mechanisms of TBN in phase II. Figure 9 presents a normalized orientation correlation function $G(t)$ in the 0 to 1.2 ps range where

$$G(t) = \frac{\int_0^\infty \frac{\varepsilon'' \cos(2\pi\tilde{\nu}ct)d\tilde{\nu}}{\tilde{\nu}[(\varepsilon' + 2\varepsilon_0)^2 + \varepsilon''^2]}}{\int_0^\infty \frac{\varepsilon'' d\tilde{\nu}}{\tilde{\nu}[(\varepsilon' + 2\varepsilon_0)^2 + \varepsilon''^2]}}$$

Plots of the orientation correlation function in the plastic and liquid phase are very similar. A slow decay of correlation is an evidence of a low reorientation rate of the molecule. An increase in temperature results in shorter relaxation times.

Such a behaviour of the correlation function in high-temperature phases is expressed by shifts of the maximum absorption with increasing temperature towards higher frequencies (Figure 7) which is characteristic of the activation processes.

In the librational phase (II) the correlation is found to decay much faster, the faster the lower is the temperature (219 K and 244 K, Figure 9). By comparing Figure 9 with plots of the orientation correlation function $G(t)$ for TBN determined by Evans[32] for various models of molecular

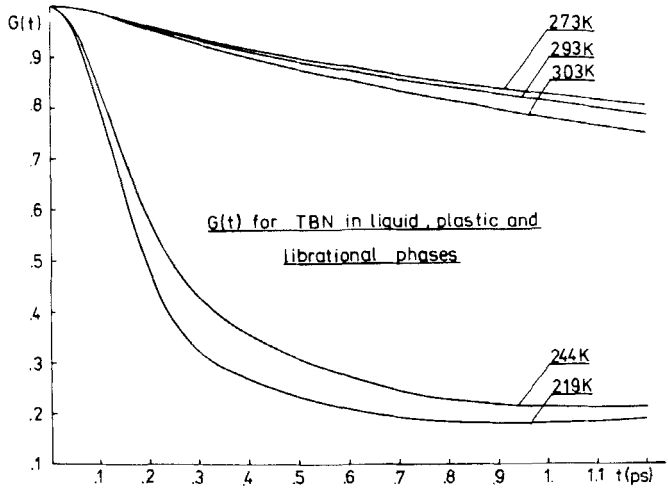


FIGURE 9 Orientational correlation function $G(t)$ for TBN in liquid phase (303 K), in phase I (273 and 293 K) and in phase II (219 and 244 K).

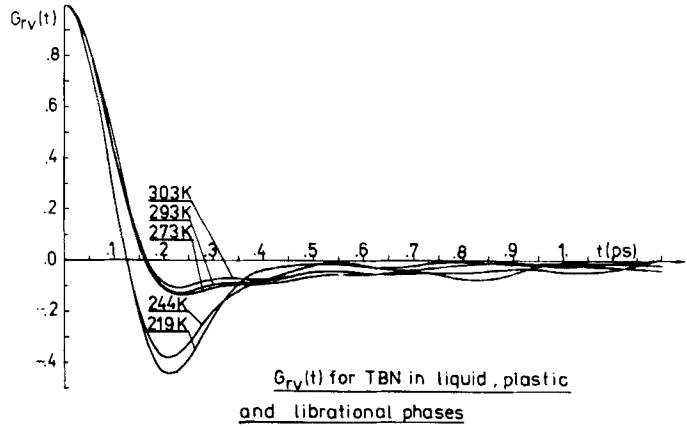


FIGURE 10 Angular velocity correlation function $G_{rv}(t)$ for TBN.

motion one can note that the experimental correlation function in this phase decays more rapidly than that calculated theoretically for a free rotator in the Mc Clung J-diffusion model.[33] This indicates that motion performed by the TBN molecule responsible for absorption in that phase could not be attributed to reorientation but these could be librations of about 0.8 ps period.

After a short time about 0.8 ps the experimental orientation correlation function in phase II reaches a constant value of 0.2–0.3 which, according to Brot,[34] is an evidence of distinguished positions in the crystal. Around these directions the molecules perform librations which presumably overlap on rapid uniaxial rotation.

For the angular velocity correlation function $G_{rv}(t)$ (Figure 10), possibilities for the distinction between two absorption mechanisms are limited, although even here the curves for phase II may be clearly separated from those for the plastic and liquid phases. Plots of the experimental $G_{rv}(t)$ are in good agreement with those determined by Evans.[35] This is quite justifiable since in the present work calculations of $G_{rv}(t)$ were performed by applying the results obtained by Haffmans and Larkin[28] as it was done by Evans.

A comparison of the experimental orientation and velocity correlation functions with the theoretical curves for the Brot–Larkin and Wyllie–Larkin model[32,35] leads to a conclusion that neither of these models corresponds fully to the results of experiments.

However, on considering the conformity of the experimental results with theoretical expectations one should have several points in mind:

i) Calculated correlation functions are the collective ones whereas the model functions do not allow for intermolecular interactions.

ii) Model correlation functions do not allow for induced absorption whose contribution, e.g. in the liquid TBN phase is estimated to be 28% of theoretical absorption. This confirms Brot's note[34] that the absence of static correlations (dipole correlation coefficient $g$ is 0.94 in this phase) does not rule out the existence of dynamic correlations.

iii) Measuring errors, particularly in band wings, which are critical for the shapes of correlation functions for short times are fairly considerable in most cases.

## References


1. C. P. Smyth, *Dielectric Phenomena.* Physics and chemistry of the organic solid state, Vol 1, Fox, Labes and Weissberger, J. Wiley, New York 1965.
2. S. Urban, Dynamical and structural aspects of molecular rotations in the $(CH_3)_3CX$ type plastic crystals. Institute of Nuclear Physics, Report no. 955/PS, Cracow, 1977 (in Polish).
3. R. H. Wiswall and C. P. Smyth, *J. Chem. Phys.*, **9**, 357 (1941).
4. L. J. Nugent, D. E. Mann, and D. R. Lide, *J. Chem. Phys.*, **36**, 965 (1962).
5. L. M. Kushner, R. W, Crowe, and C. P. Smyth, *J. Am. Chem. Soc.*, **72**, 1091 (1950).
6. A. Dvorkin and M. Guillamin, *J. Chem. Phys.*, **63**, 53 (1966).
7. S. Urban, Z. Tomkowicz, J. Mayer, and T. Waluga, *Acta Phys. Pol.*, **A48**, 61 (1975).
8. E. F. Westrum and A. Ribner, *J. Phys. Chem.*, **71**, 1216 (1967).
9. R. M. Rudman and B. Post, *Mol. Crystals*, **5**, 95 (1968).
10. R. S. Schwartz, B. Post, and I. Fankuchen, *J. Am. Chem. Soc.*, **73**, 4490 (1951).
11. J. Mayer, I. Natkaniec, J. Sciesiński, and S. Urban, *Acta Phys. Pol.*, **A52**, 665 (1977).
12. A. I. Kitaigorodsky, *Molecular Crystals and Molecules*, Academic Press, New York, London, 1973.
13. S. Urban, J. A. Janik, J. Lenik, J. Mayer, and T. Waluga, *Phys. Stat. Sol.*, **A10**, 271 (1972).
14. Abhai Mansingh and D. B. McLay, *Can. J. Phys.*, **45**, 3815 (1967).
15. S. Urban, J. Lenik, J. Mościcki, and S. Wróbel, *Acta Phys. Pol.*, **A48**, 787 (1975).
16. P. Freundlich, J. Kalenik, E. Narewski, and L. Sobczyk, *Acta Phys. Pol.*, **A48**, 701 (1975).
17. K. Czarniecka, A. Jaich, P. Freundlich, and S. Urban, *Acta Phys. Pol.*, **A57**, 679 (1980).
18. D. Schmid and U. Wannagat, *Chem. Zeitung*, **98**, 575 (1974).
19. H. Hänsel, Grundzüge der Fehlerrechnung, WNT, Warszawa, 1968, Polish translation.
20. H. A. Kolodziej, M. Pajdowska, and L. Sobczyk, *J. Phys. E.*, **11**, 752 (1978).
21. F. Buckley and A. A. Maryott, Tables of dielectric dispersion data for pure liquids and dilute solution. Nat. Bureau of Standards, Washington, 1958.
22. A. R. von Hippel, *Dielectric Materials and Applications*, J. Wiley, 1958.
23. C. Clemett and M. Davies, *Trans. Faraday Soc.*, **58**, 1705 (1962).
24. R. W. Crowe and C. P. Smyth, *J. Am. Chem. Soc.*, **72**, 4009 (1950).
25. S. Urban, *Acta Phys. Pol.*, **A49**, 741 (1976).
26. R. J. Meakins, *Mechanism of Dielectric Absorption in Solids.* Progress in dielectrics, ed. J. B. Birks, Vol. 3 (1961).
27. H. Fröhlich, *Theory of Dielectrics*, Clarendon Press, Oxford, 1958.
28. R. Haffmans and I. W. Larkin, *JCS Faraday Trans. II*, **68**, 1729 (1972),
29. H. Fröhlich, *Trans. Faraday Soc.*, **42A**, 3 (1946).
30. E. Bauer and D. Massignon, *Trans. Faraday Soc.*, **42A**, 12 (1946).
31. J. P. Hawranek, P. Neelakantan, R. P. Young, and R. N. Jones, *Spectrochim. Acta*, **32A**, 85 (1976).
32. M. Evans, *JCS Faraday Trans. II*, **72**, 727 (1976).
33. R. E. D. McClung, *J. Chem. Phys.*, **57**, 5478 (1972).
34. C. Brot, *Correlation Functions in Dipolar Absorption-Dispersion.* Dielectric and related molecular processes, ed. M. Davies, Vol. 2, The Chemical Society, London, 1974.
35. M. Evans, *JCS Faraday Trans. II*, **71**, 2051 (1976).